Final submitted version of:
Le Toan, T., Quegan, S., Davidson, M., Balzter, H., Paillou, P., Papathanassiou, K., Plummer, S., Rocca, F., Saatchi, S., Shugart, H. and Ulander, L. (2011)*:* The BIOMASS Mission: Mapping global forest biomass to better understand the terrestrial carbon cycle, *Remote Sensing of Environment* 115 2850– 2860.

The BIOMASS Mission: Mapping global forest biomass to better understand the terrestrial carbon cycle

T. Le Toan[1], S. Quegan[2], M. W.J. Davidson[3], H. Balzter[4], P. Paillou[5], K. Papathanassiou[6], S. Plummer[7], F. Rocca[8], S. Saatchi[9], H. Shugart[10], L. Ulander[11]

1. Centre d'Etudes Spatiales de la Biosphère, CNRS-CNES-Université Paul Sabatier-IRD, Toulouse, France
2. Centre for Terrestrial Carbon Dynamics (CTCD), University of Sheffield, UK
3. Mission Science Division, ESA- ESTEC, the Netherlands
4. Centre for Environmental Research (CERES), University of Leicester, UK
5. Observatoire Aquitain des Sciences de l'Univers, Université Bordeaux-1, France
6. German Aerospace Center e.V. (DLR), Wessling, Germany
7. IGBP-ESA Joint Projects Office, ESA-ESRIN, Italy
8. Dipartimento di Elettronica ed Informazione, Politecnico di Milano, Italy
9. Jet Propulsion Laboratory, Pasadena, USA
10. University of Virginia, Charlottesville, Virginia USA
11. Department of Radar Systems , FOI, Linkoping, Sweden

Corresponding author

Thuy Le Toan

Tel : +33 5 61 55 66 71 Fax : + 33 5 61 55 85 00

Email : Thuy.Letoan@cesbio.cnes.fr

Abstract

Knowledge about above-ground forest biomass is of fundamental importance in quantifying the terrestrial carbon cycle. It is also an essential element in assessing terrestrial carbon fluxes under the United Nations Framework Convention on Climate Change and is crucial in assessing both resources and the ecosystem services provided by forests. For most parts of the world, in particular the tropical forests, information on biomass is currently very limited. It is usually resolved at very coarse scales, and is subject to large and unquantified errors. In response to the urgent need for improved mapping of global biomass and the lack of any current space systems capable of addressing this need, the BIOMASS mission was proposed to the European Space Agency for the third cycle of Earth Explorer Core missions and was selected for Feasibility Study (Phase A) in March 2009. Over the five-year mission lifetime, it will map the full range of the world's above-ground biomass with accuracy and spatial resolution compatible with the needs of national scale inventory and carbon flux calculations, and will map changes in forest biomass. The mission will carry a polarimetric P-Band SAR, capable of providing both direct measurements of biomass derived from inverting intensity data, and measurements of forest height derived from polarimetric interferometry. This paper describes the characteristics of the mission and surveys the body of evidence built up over the last decade, from a wide range of airborne experiments, which illustrates the ability of such a sensor to provide the required measurements. It also indicates the likely value of the mission to several other

geo-science areas, including geomorphology in arid areas, ice structure and dynamics, and the dynamics of forest inundation.

1. Introduction - Biomass and the global carbon cycle

One of the most unequivocal indications of man's effect on our planet is the continual and accelerating growth of carbon dioxide (CO_2) in the atmosphere. A central concern is the climate-change implication of increasing atmospheric CO_2. The principal contribution to this growth is emissions from fossil fuel burning. However, the rate of growth is substantially less and much more variable than these emissions because of a net flux of CO_2 from the atmosphere to the Earth's surface. This net flux can be partitioned into atmosphere-ocean and atmosphere-land components, whose mean values for the 1990s are 2.2 ± 0.4 GtC y^{-1} and 1.0 ± 0.6 GtC y^{-1} respectively (International Panel on Climate Change (IPCC), 2007). As in most carbon cycle calculations, CO_2 fluxes are reported in this paper in terms of carbon units; 1 GtC = 1 Pg or10^{15} g of carbon.

This simple description of the overall carbon balance conceals some major scientific issues, which we illustrate by Fig. 1:

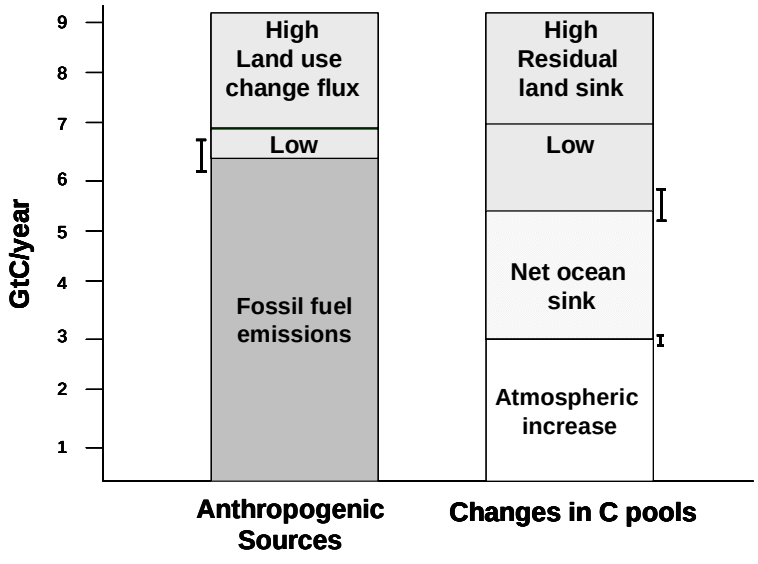

Figure1. *Bar chart showing the anthropogenic carbon sources and the associated annual net fluxes to the carbon pools for the 1990s, with units given as GtC* yr^{-1}. *The uncertainties in the well-constrained terms (fossil fuel emissions, the atmospheric increase in* CO_2 *and the net ocean sink) are indicated by the error bars. The land use change flux is poorly constrained and the chart indicates the range of estimates, from low to high, of this quantity. In order to achieve carbon balance, there must be take-up of* CO_2 *by the land surface, and the corresponding low and high estimates of this "residual land sink" are indicated. The data for this figure are taken from IPCC (2007).*

1. Although fossil fuel emissions, the atmospheric CO_2 increase and the net atmosphere-ocean flux are well constrained by measurements (IPCC, 2007), this is not true of the atmosphere-land flux. Its value is estimated simply as the residual needed to close the carbon budget after subtracting the atmospheric growth in CO_2 and the net amount transferred into the oceans from the emissions. Hence its variance is determined indirectly as the sum of the variances of the other fluxes.

2. Fossil fuel burning forms only part of the total anthropogenic CO_2 loading of the atmosphere, with another major contribution coming from land use change. The size of this flux is poorly known, and is reported in IPCC (2007) simply as a range, shown in Fig. 1 as a low and high value about a central value of 1.6 GtC y^{-1}. (It is worth noting that the lastest value put it to 1.4 GtC y^{-1} (Le Quéré et al., 2009)).

3. In order to balance the carbon budget, any value of land-use-change flux must have an associated land uptake flux, indicated in Fig. 1 as a "residual" flux, since its value is derived purely as a difference of other terms.

Marked on Fig. 1 are the uncertainties in the well-constrained terms; it can be seen that the uncertainties in both emissions and uptake by the land dominate the overall error budget. Fundamental to better quantification of these land fluxes is accurate knowledge about the magnitude, spatial distribution and change of forest biomass.

More than 98% of the land-use-change flux is caused by tropical deforestation (IPCC, 2007), which converts carbon stored as woody biomass (which is approximately 50% carbon) into emissions. The most basic methods of calculating this flux simply multiply the area deforested (derived from national statistics or remote sensing) by the average biomass of the deforested area, expressed in carbon units (IPCC, 2003). More complete methods of carbon accounting would include carbon fluxes from the soil, differential decay rates of carbon depending on how the biomass is used, and regrowth fluxes (Houghton, 2003a, b; DeFries et al., 2002). However, both approaches are severely compromised by lack of reliable information on the levels of biomass actually being lost in deforestation. This uncertainty alone accounts for a spread of values of about 1 GtC y^{-1} in different estimates of carbon emissions due to tropical deforestation (Houghton, 2005).

The residual land flux is of major significance for climate, since it reduces the build-up of CO_2 in the atmosphere. If we assume a land use change flux of 1.6 GtC yr^{-1}, the total anthropogenic flux to the atmosphere in the 1990s was 8 GtC yr^{-1}. Of this, around 32.5% was absorbed by the land (see Fig. 1), but this value has very large uncertainties arising from the uncertainties in the land use change flux. The uptake is highly variable from year to year, for reasons that are poorly understood. Similar trends are seen since 2000 (Canadell et al., 2007). A key question is how much of this residual sink is due to fixing of carbon in forest biomass.

As a result, biomass is identified by the United Nations Framework Convention on Climate Change (UNFCCC) as an Essential Climate Variable (ECV) needed to reduce uncertainties in our knowledge of the climate system (GCOS 2003; Sessa and Dolman, 2008). Further strong impetus to improve methods for measuring global biomass comes from the Reduction of Emissions due to Deforestation and Forest Degradation (REDD) mechanism, which was introduced in the UNFCCC Committee of the Parties (COP-13) Bali Action Plan. Its implementation relies fundamentally on systems to monitor carbon emissions due to loss of biomass from deforestation and forest degradation.

Concerns about climate change provide a compelling reason for acquiring improved information on biomass, but biomass is also profoundly important as a source of energy and materials for human use. It is a major energy source in subsistence economies, contributing around 9-13% of the global supply of energy (i.e. 35-55 $\times 10^{18}$ Joule yr^{-1}; Haberl and Erb, 2006). The FAO provides the most widely used information source on biomass harvest (FAO, 2001; FAO 2006), but other studies differ from the FAO estimates of the wood-fuel harvest and forest energy potential by a factor 2 or more (Whiteman et al., 2002, Smeets et al., 2007; Krausmann et al., 2008). Reducing these large uncertainties requires frequently updated information on woody biomass stocks and their change over time, to be combined with other data on human populations and socio-economic indicators.

Biomass and biomass change also act as indicators of other ecosystem services. Field studies have shown how large-scale and rapid change in the dynamics and biomass of tropical forests lead to forest fragmentation and increase in the vulnerability of plants and animals to fires (Malhi and Phillips, 2004). Bunker et al. (2005) also showed that above-ground biomass was strongly related to biodiversity. Regional to global information on human impacts on biodiversity therefore requires accurate

determination of forest structure and forest degradation, especially in areas of fragmented forest cover. This is also fundamental for ecological conservation. The provision of regular, consistent, high-resolution mapping of biomass and its changes would be a major step towards meeting this information need.

Despite the obvious need for biomass information, and in contrast with most of the other terrestrial ECVs for which programmes are advanced or evolving, there is currently no global observation programme for biomass (Herold et al., 2007). Until now, the only sources of gridded global biomass (i.e. typically above-ground biomass, which is the dry weight of woody and foliar tree elements) are maps at very coarse spatial resolutions (1/2 to 1 degree) based largely on ground data of unknown accuracy (Olson et al., 1983; Olson et al., 2001; Kindermann et al., 2008). At regional scale, various approaches have been used to produce biomass maps. Houghton et al. (2003) compared seven biomass maps of the Brazilian Amazon forest produced by different methods, including interpolation of in situ field measurements, modelled relationships between above-ground biomass and environmental parameters, and the use of optical satellite data to guide biomass estimates. In these maps, estimates of the total amount of carbon in the Brazilian Amazon forests varied from 39 to 93 Gt of carbon, and the correlation between the spatial distributions of biomass in the various maps was only slightly better than would be expected by chance (Houghton et al., 2003).

Currently, there are severe limitations on the use of remote sensing to measure biomass. Optical data are not physically related to biomass, although estimates of biomass have been obtained from Leaf Area Index (LAI) derived from optical greenness indices. However, these are neither robust nor meaningful above a low value of LAI. For example, Myneni et al. (2001) used optical data from the Advanced Very High Resolution Radiometer (AVHRR) sensors to infer biomass changes in northern forests

over the period 1981-1999, and concluded that Eurasia was a large sink. However, both field data and vegetation models indicate that the Eurasian sink is much weaker (Beer et al., 2006). Radar measurements, resulting from the interaction of the radar waves with tree scattering elements, are more physically related to biomass, but their sensitivity to forest biomass depends on the radar frequency. C-band (ERS, Radarsat and ENVISAT ASAR) backscatter in general shows little dependence on forest biomass. C-band interferometric measurements do better; for example, ERS Tandem data were combined with JERS L-band data to generate a map of biomass up to 40-50 t ha^{-1} with 50 m pixels covering 800000 km^2 of central Siberia (Schmullius et al., 2001). From the more recent Advanced Land Observing Satellite (ALOS) mission, launched by the Japan Aerospace Exploration Agency (JAXA) in 2006, Phased Array L-band SAR (PALSAR) data are being systematically collected to cover the major forest biomes. Recent results (http://www.ies.aber.ac.uk/en/subsites/the-alos-kyoto-amp-carbon-initiative) have shown PALSAR's ability to map forest (e.g. in the Amazon and Siberia) but retrieval of forest biomass is still typically limited to values less than 50 t ha^{-1}, which excludes most temperate and tropical forests. Furthermore, loss of temporal coherence over the PALSAR repeat interval of 45 days prevents recovery of forest height by polarimetric SAR interferometry.

It is against this background of an urgent need for greatly improved mapping of global biomass and the lack of any current space systems capable of addressing this need that the BIOMASS mission was proposed to the Call for Ideas released in March 2005 by the European Space Agency (ESA) for the third cycle of Earth Explorer Core missions. BIOMASS was selected in May 2006 for Assessment Study (phase 0) and in March 2009 for Feasibility Study (phase A). This paper identifies the issues of concern addressed by the mission, summarises its specific research objectives, and specifies the

observational requirements within the context of the scientific objectives. Finally, a short overview of the mission elements is given.

2. The BIOMASS mission

The primary scientific objectives and characteristics of the BIOMASS mission are set out in Table 1. It will carry a polarimetric P-Band SAR that will provide:

- Measurements of the full range of the world's above-ground biomass, by combining several complementary SAR measurement techniques;
- Geophysical products whose accuracy and spatial resolution are compatible with the needs of national scale inventory and carbon flux calculations;
- Repeated global forest coverage, enabling mapping of forest biomass and forest biomass change.

By making these measurements over the proposed five-year mission lifetime, a unique archive of information about the world's forests and their dynamics will be built up, which will have lasting value well beyond the end of the mission.

The P-band frequency was chosen because of its unique capabilities for forest biomass and height measurement. Sensitivity to forest biomass and biomass change increases with wavelength (Le Toan et al., 1992, Dobson et al., 1992, Le Toan et al., 2004). In addition, longer wavelength SAR exhibits greater temporal coherence, allowing canopy height to be retrieved by polarimetric interferometry; this is a crucial complement to methods that recover biomass by inverting SAR intensity data. Both considerations strongly support the use of P-band, since it is the longest wavelength available for spaceborne application.

The opportunity to use P-band arose only when the International Telecommunications Union (ITU) designated the frequency range 432-438 MHz as a secondary allocation to remote sensing at the World Radio Communications Conference in 2003 (ITU, 2004). The BIOMASS SAR will therefore operate at a centre frequency of 435 MHz (i.e., a wavelength of around 69 cm) and with a bandwidth of 6 MHz.

Table 1*: BIOMASS primary science objectives and mission requirements.*

Primary science objectives	**Measurement requirements**	**Instrument requirements**
Quantify magnitude and distribution of forest biomass globally to improve resource assessment, carbon accounting and carbon models	Above-ground forest biomass from 70^{o} N to 56^{o} S with accuracy of ±20% (or classes of 10 t ha^{-1} in forest regrowth) at spatial scale of 100-200 m. Forest height with accuracy of ±4 m. Forest mapping at spatial scales of 100-200 m.	P-band SAR (432-438 MHz) Polarimetry for biomass retrieval and ionospheric correction Pol-InSAR capability to measure forest height Constant incidence angle (in the range of 23^{o}-35^{o}) 25-45 day repeat cycle for interferometry Dawn-dusk orbit to reduce ionospheric effects 1 dB absolute accuracy in intensity measurements 0.5 dB relative accuracy in intensity measurements 5 year mission lifetime
Monitor and quantify changes in terrestrial forest biomass globally, leading to improved estimates of: (a) terrestrial carbon sources (primarily from deforestation) using accounting methods; (b) terrestrial carbon sinks due to forest regrowth and afforestation	Biomass loss due to deforestation and forest degradation, annually or better, at spatial scales of 100-200 m. Biomass accumulation from forest growth, at spatial scale of 100-200 m; 1 estimate per yr in tropical forests, 1 estimate over 5 yrs in other forests. Changes in forest height caused by deforestation. Changes in forest area at spatial scales of 100-200 m, annually or better.	

3 Forest biomass retrieval using P-band SAR

The various approaches to recovering forest biomass from P-band SAR data are summarised in this section.

3.1 Forest biomass retrieval using radar backscattering coefficients

The sensitivity of P-band SAR backscatter to forest biomass has been studied since the first airborne P-band systems became available in the early 1990s. Numerous airborne campaigns have taken place, over a wide variety of forest biomes, including sites in temperate, tropical and boreal forests. Most initial work focused on the cross-polarised Horizontal-Vertical (HV) backscatter, which has the largest dynamic range and the highest correlation with biomass. Fig. 2 illustrates the key characteristics of the observed relationship between forest biomass and the HV radar backscattering coefficient. The data come from several different forest types, including temperate coniferous forest in Les Landes, France (Le Toan et al., 1992, Beaudoin et al., 1994); boreal forest with mixed species in Alaska, USA (Rignot et al., 1994); northern temperate forest with mixed species in Howland, Maine, USA (Ranson et al. 1994); tropical forest in Guaviare, Colombia (Hoekman et al., 2000); tropical forest in La Selva, Costa Rica (Saatchi et al., 2009); and hemi-boreal coniferous and deciduous forest in Remningstorp, Sweden (Sandberg et al., 2009).

The SAR data were all acquired by the NASA-JPL AIRSAR system, except those from Sweden, which were acquired by the E-SAR system from DLR, Germany.

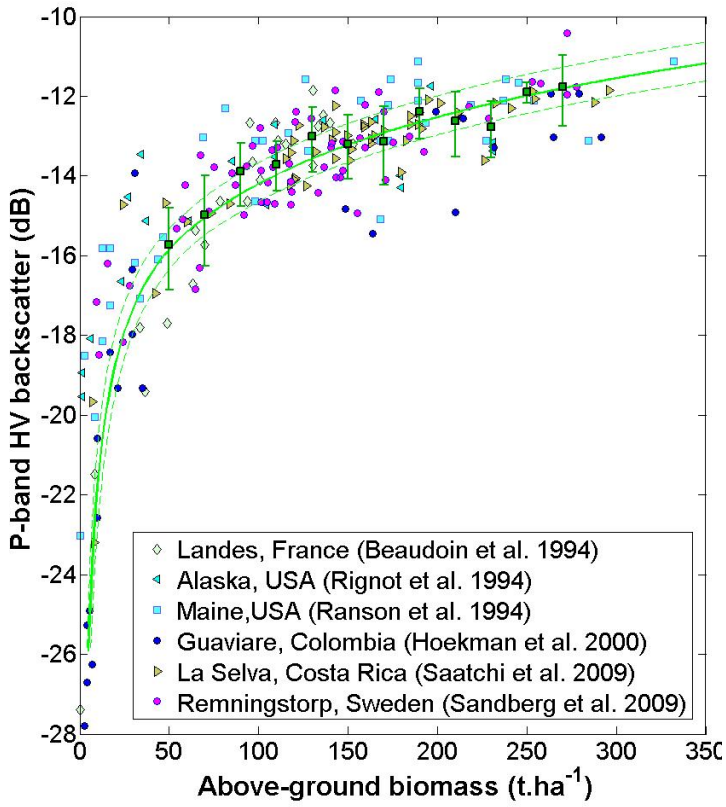

Figure 2. *P-band HV backscattering coefficient plotted against above-ground biomass for experiments conducted at six different forests as indicated in the key. The backscattering coefficient is expressed as* $\gamma^0_{HV} = \sigma^0_{HV}/\cos\theta$, *where* θ *is the incidence angle. The green squares with error bars indicate the mean and standard deviation of the data points within intervals of* ± 10 *t ha*$^{-1}$ *centred on values of biomass spaced by 20 t ha*$^{-1}$, *beginning from 50 t ha*$^{-1}$ *and running out to 270 t ha*$^{-1}$. *The solid green line is a regression curve derived from the combined data reported in the publications prior to 2009. The dashed curves are obtained by replacing the biomass value, B, by* $0.8\times B$ and $1.2\times B$ *in the regression equation.*

Fig 2 shows the HV backscattering coefficient (expressed in terms of $\gamma^0_{HV} = \sigma^0_{HV}/\cos\theta$, where θ is the incidence angle, to provide a first order correction for different incidence angles in the various datasets) plotted against ground-based estimates of biomass. The data acquired in the 1990s were used to derive the solid green fitting

curve shown in Figure 2. For the two more recent datasets (La Selva and Remningstorp), constants of + 5 dB and - 3 dB, respectively (estimated to give the least root mean square (RMS) error with the fitting curve) were added to the backscatter values to compensate for the observed offsets from the earlier datasets and attributed to absolute calibration uncertainties in the airborne instruments. The dashed green curves delimit the ± 20% uncertainties in *in situ* biomass around the fitting curve, obtained by replacing the biomass value B by $0.8 \times B$ and $1.2 \times B$. The green squares with error bars indicate the mean and standard deviation of the data points within intervals of ± 10 t ha^{-1} centred on values of biomass spaced by 20 t ha^{-1}, beginning from 50 t ha^{-1} and running out to 270 t ha^{-1}.

Fig. 2 indicates a remarkable consistency in the shape of the biomass-HV backscatter relationship over this varied set of forest biomes, despite variability in the measurements caused by: (a) errors in the in situ estimates of forest biomass; (b) errors in the estimates of the radar backscattering coefficient (due to speckle, calibration and geolocation errors); and (c) "geophysical" variability due to forest characteristics (e.g., species, number density, age class), as well as to topography, weather conditions and understorey conditions. Among these sources of error, the error associated to *in situ* biomass estimates can contribute significantly to the scatter observed in Fig. 2. In practical forestry, the uncertainty in biomass estimates is usually estimated to be about ~20%, based on stand-based timber volume for even-aged plantation forests (Le Toan et al., 1992). However, for most forests in natural condition, the error in biomass estimates can be much larger due to : (i) the choice of allometric models relating biomass to measured tree dimensions; (ii) the sampling uncertainty, related to the size and representativeness of the measurement plots; (iii) the error in wood density needed to convert timber volume into biomass and iv) the exclusion of small trees (e.g. those of diameters less than 10 cm, 7 cm or 5 cm depending on measurement standards). In an analysis of uncertainty sources for a tropical forest Chave et al., 2005, found that the uncertainty in *in situ* biomass estimate is of 24%

of the mean for measurement plot of 1 ha, and it increases reversely with the size of the measurement plot. Hence, for the general case where measurement plots are much smaller than 1 ha, the uncertainty in *in situ* biomass estimates can be considered as much larger than ~25% of the mean.

It can be seen that the HV backscatter increases by over 17 dB as biomass ranges from a few t ha-1 up to 300 t ha-1. Such a large contrast between high and low biomass areas allows major disturbances, such as clear-felling of forests, to be easily detected. The sensitivity of backscatter to biomass is greatest at lower values of biomass, up to about 150 t ha-1, and enables the early years of regrowth after disturbance to be monitored.

The observed relationship between P-band backscatter and biomass has been interpreted using electromagnetic scattering models (Ulaby et al., 1990; Hsu et al., 1994; Fung, 1994; Ferrazzoli et al., 1997). These studies found that HV backscatter is dominated by volume scattering from the woody elements in the trees, so that HV is strongly related to the above-ground biomass. For the HH and VV polarisations, ground conditions can affect the biomass-backscatter relationship, because HH backscatter comes mainly from trunk-ground scattering, while VV backscatter results from both volume and ground scattering. At present, biomass retrieval from multiple polarisations has been achieved by regression on a quadratic form, developed to simplify the complex modelling formulation (Saatchi et al. 2007). The inversion requires forest training plots for model calibration and also information on topography, since HH is affected by ground conditions.

Errors in estimates of biomass by inverting either the HV backscatter alone or HV with other polarisations vary between studies, and depend on the range of biomass and the methods used to estimate in situ biomass. Reported RMS errors in literature (e.g. Le Toan et al., 1992, Beaudoin et al., 1994); Rignot et al., 1994; Ranson et al. 1994); Hoekman et al., 2000; Saatchi et al., 2009; and Sandberg et al., 2009) fall in the range 15% to 35% of the mean biomass, with higher values at the test-sites with larger ranges of biomass.

Fig. 3 shows the biomass map for a section of the Landes forest, estimated by inverting the HV backscatter, together with a scatterplot of *in situ* measurements of biomass for twelve reference forest stands plotted against values estimated by inversion. This forest has very homogenous stands with biomass in the range 0-150 t ha^{-1}, and inverting HV backscatter alone yields an RMS error of less than 10 t ha^{-1}. For more complex forests, e.g. with more heterogeneity and a larger biomass range, inversion of HV intensity using the empirical curve in Fig. 2 is expected to yield larger errors. This is illustrated by the image and scatterplot in Fig. 4 for the Remningstorp site. Comparing the mean biomass at 55 reference stands with the biomass values obtained by *in situ* measurements and derived from laser height estimates, as described in Sandberg et al. (2009), gives an RMS inversion error of 47 t ha^{-1}.

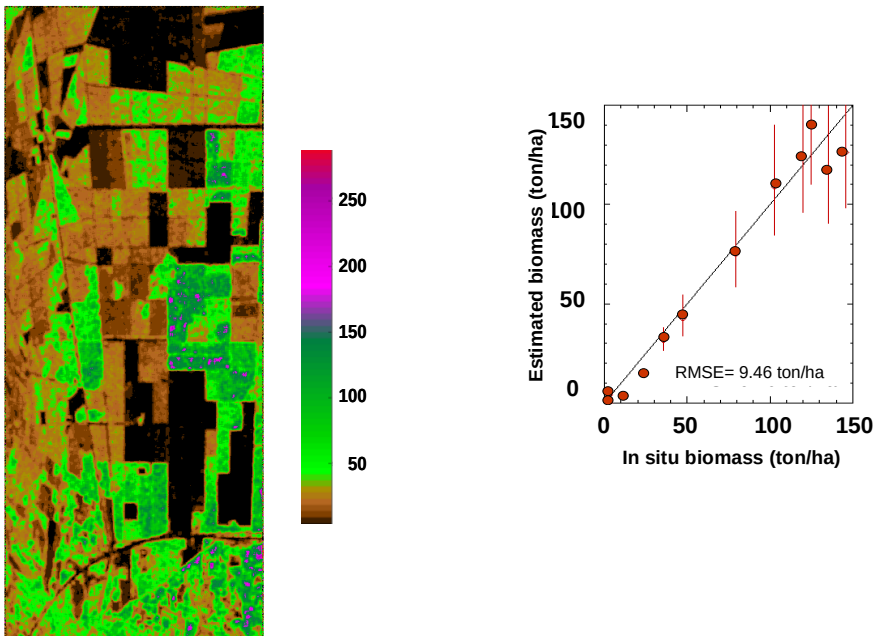

Figure 3. Left: *Map of biomass for a section of the Landes forest (about 3.5 km x 9.5 km) based on inverting the HV backscatter measured by AirSAR.* Right: *Comparisons between ground-based measurements of biomass and backscatter inversion for twelve reference stands.*

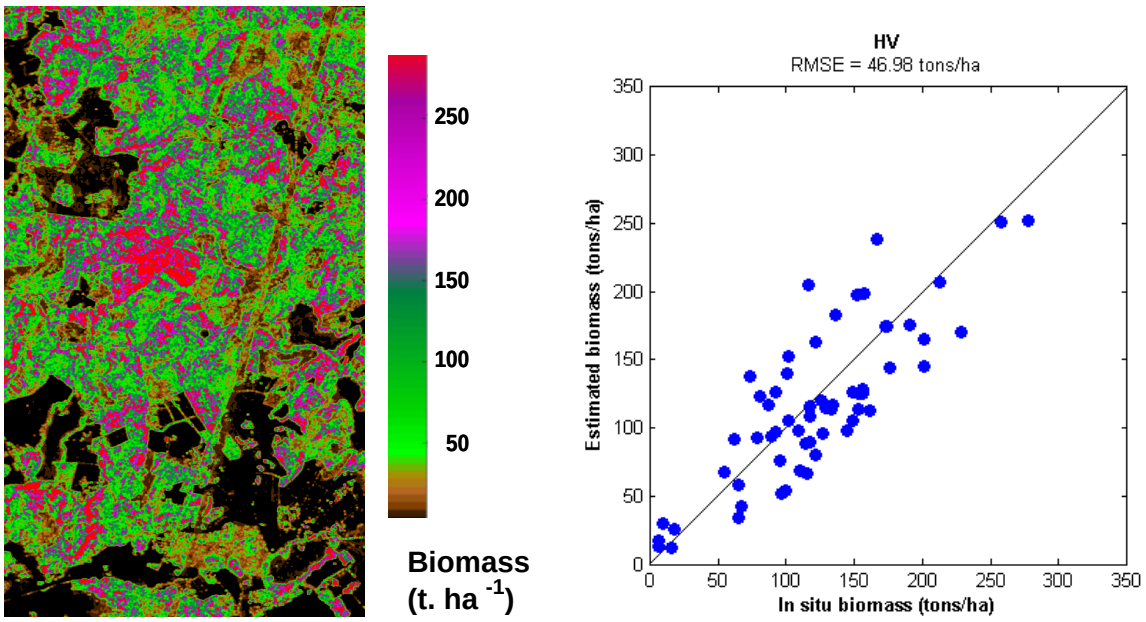

Figure 4. Left: *Map of biomass for a section of the Remningstorp forest (about 3.4 km x 5.7 km) based on inverting HV backscatter measured by E-SAR. Right: Comparisons between biomass derived from backscatter inversion and biomass data at 55 reference stands.*

3.2 Improving biomass estimates by using polarimetric interferometry

Because the sensitivity of the backscattering coefficient to biomass decreases at high levels of biomass, inversion methods based solely on intensity are insufficient to cover the full range of the world's biomass. For example, old growth forest plots in the Amazon forest have biomass in the range 200-400 t ha^{-1} (Malhi et al., 2006). However, the use of polarimetry and forest vertical structure from interferometry will potentially improve the biomass estimation in the so-called "saturation" region. This can be achieved by measuring forest height using a SAR technique known as polarimetric interferometry or Pol-InSAR (Cloude et al., 2001). A major advantage of this approach is that both height and biomass measurements are provided independently by the same

radar sensor. In addition, the sensitivity of Pol-InSAR to height *increases* with height (and hence biomass), whereas the sensitivity of intensity to biomass *decreases* with biomass, so that the two measurements complement each other when used jointly in retrieval.

3.2.1 Measurement of forest height using Pol-InSAR

The key quantity measured by Pol-InSAR is the interferometric coherence, γ, which is the modulus of the complex correlation coefficient between two images of a scene acquired at different times (for a repeat pass system) and with slightly different geometries. The coherence can be decomposed into three main contributions:

$$\gamma = \gamma_{SNR}\, \gamma_t\, \gamma_{vol}\,. \qquad (4)$$

The noise decorrelation (γ_{SNR}) is of secondary importance in forest observations, so the two important terms are the temporal coherence (γ_t), which measures the stability of the scatterers between the two acquisitions, and the volume decorrelation (γ_{vol}). The latter is related to the vertical distribution of scatterers, *F(z)*, also known as the vertical structure function, where *z* is height, through a Fourier Transform relationship. It is therefore a key observable for quantitative forest parameter estimation (Treuhaft and Siqueira, 2000; Askne et al., 1997; Cloude and Papathanassiou, 1998; Papathanassiou and Cloude, 2001), and height retrieval from Pol-InSAR is based on estimating this quantity.

An important special case of *F(z)* is the exponential profile which, when combined with a delta function for the ground contribution, forms the basis for the widely-used Random-Volume-over-Ground (RVoG) model (Cloude and Papathanassiou 2003). Despite its simplicity, this model has been successfully used to estimate forest height from L- and P-band coherence in experiments in temperate forests (Papathanassiou and

Cloude, 2001; Mette et al., 2004; Dubois-Fernandez et al., 2008; Garestier et al., 2008a, 2008b; Garestier and Le Toan, 2009a, 2009 b), boreal forests (Praks et al., 2006; Lee at al., 2008) and tropical forests (Kugler et al., 2006; Kugler et al., 2007; Hajnsek et al., 2008). Height errors in the P-band retrievals were typically found to be around 2 to 4 m.

Of great importance is that Pol-InSAR methods have been demonstrated in tropical forests, as illustrated by Fig. 5. This shows a height map of the Mawas region, Indonesia, derived from P-band data acquired during the ESA Indrex campaign in 2004, and a comparison between radar-derived and lidar measurements of H_{100} along a transect crossing the site. The RMS difference between the two height measurements is 1.73 m over heights ranging from 4 to 27 m (Hajnsek et al., 2009).

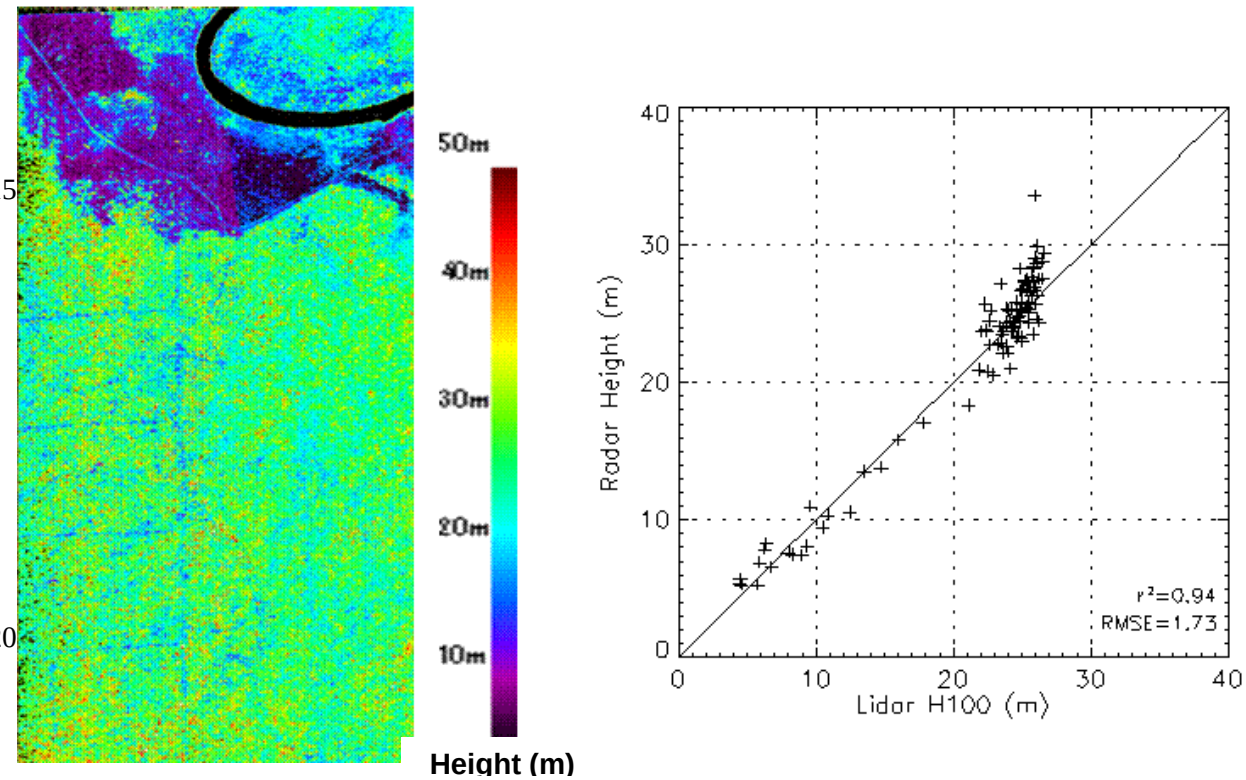

Figure 5. Left: *Pol-InSAR height map for tropical forest at the Mawas test site, Indonesia, produced using data from the E-SAR system in the ESA Indrex experiment.*

Right: *Comparison between P-band Pol-InSAR height and lidar height (Hanjsek et al., 2008).*

A critical issue for repeat-pass spaceborne Pol-InSAR measurements is temporal decorrelation caused by changes in the scene occurring between acquisitions. This is because Pol-InSAR interprets temporal decorrelation as volume decorrelation (see eq. (4)), which biases the height estimates and increases their dispersion (Lee at al., 2008). A fundamental advantage of P-band over higher radar frequencies is that it has much greater resistance to temporal decorrelation, firstly because P-band backscatter tends to come from large tree elements (the trunk and big branches) which are inherently very stable and secondly because scatterer motions of a given magnitude have much less impact on P band. This is illustrated in Fig. 6, which shows a simulation, based on a formulation by Zebker and Villasenor (1992), of the effect of scatterer motion on coherence as a function of wavelength; the range of wavelengths covered by SAR systems operating at C-, L- and P-band is also indicated. In this simulation, the scatterers are assumed to be the same for all frequencies and to suffer independent Gaussian displacements with standard deviation 1, 3 and 5 cm between acquisitions. Although an idealization, the plot clearly indicates that lower frequencies are much less sensitive to motion-induced decorrelation. Motions of 1 cm have little effect on P-band coherence, and are tolerable at L-band, but destroy C-band coherence. Motions of 3 cm reduce the P-band coherence by around 0.1, but the L-band coherence is reduced to a level that makes it unusable for height estimation. When motions grow to 5 cm, height biases at L- and P-band are too large for the measurements to be useful.

These properties are highlighted by Fig. 7, which shows the height and height error obtained from the inversion of single-baseline fully polarimetric ESAR Pol-InSAR data using the RVoG model for the Remningstorp test site. Note that this is the same scene as in Fig. 4. Fig. 7a shows the height map at P-band obtained from quasi-simultaneous acquisitions and is derived without using a priori information about terrain or vegetation density (Cloude & Papathanassiou 2003, Hajnsek et al. 2009). Fig. 7b shows the corresponding height error at P-

band obtained from acquisitions separated by 30 days. Biases introduced by temporal decorrelation are seen to be generally small (a few m) at P band, but can exceed 20 m at L band for the same temporal baseline (see Fig. 7c).

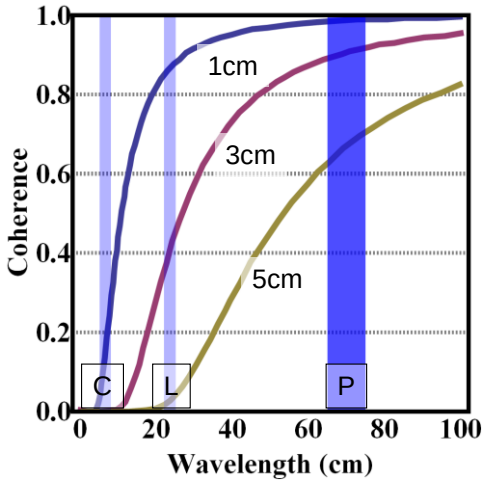

Figure 6. *Simulated effect on coherence of scatterer motions of RMS magnitudes 1, 3 and 5 cm as a function of wavelength, together with the range of wavelengths covered by SAR systems operating at C-, L- and P-band.*

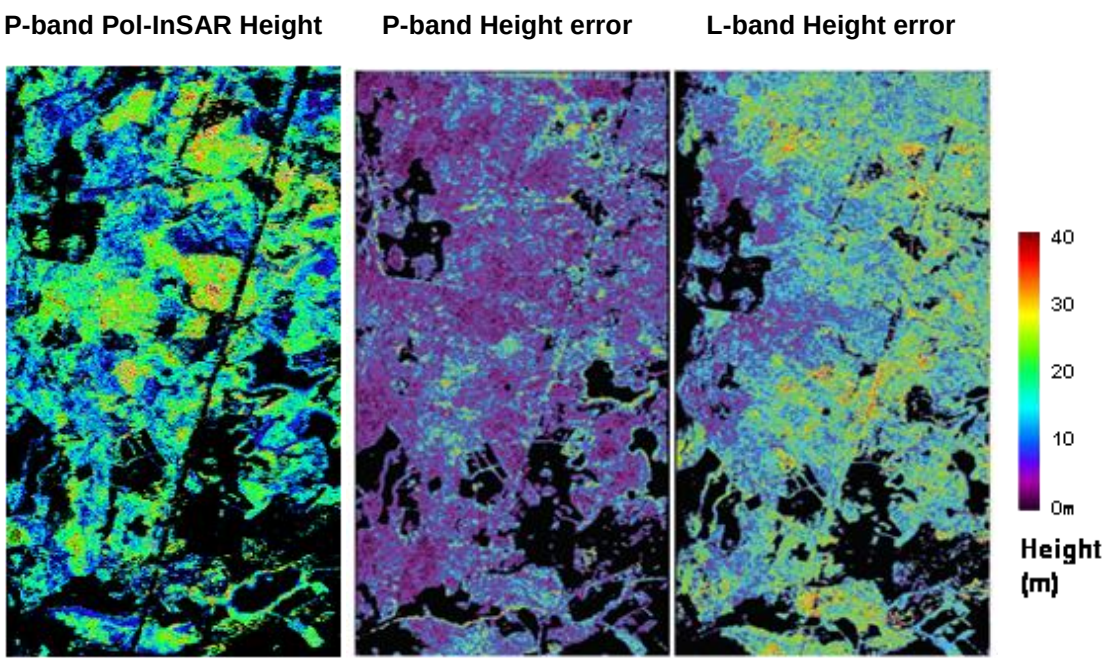

(a) (b) (c)

Figure 7*: (a) Height map derived from P-band Pol-InSAR for the Remningstorp test site) Errors in estimates of height derived from 30-day coherence by Pol-InSAR techniques at P- and L-band are shown in (b) and (c) respectively.*

3.2.2 Allometric relations between biomass and forest height

The importance of height in estimating biomass comes from the key theoretical relationship that, for a given species, the two are related by a power law:

$$B \propto H^{\alpha}, \qquad (2)$$

where B is above-ground biomass and H is an estimate of height, and where variations in the exponent α are mainly due to natural or artificial thinning (Woodhouse, 2006). Equations of this form have been developed for trees in different forest zones, with α ranging from 0 to 4. For example, for four common European forest species (spruce, pine, oak and beech), Mette (2007) found the relation

$$B = 0.801 \times H_{100}^{\,1.748} \qquad (3)$$

Where B is biomass in t ha $^{-1}$, H_{100} denotes top height in metre, defined as the mean height of the 100 trees with the largest diameter in a 1 ha area. For most forests, the value of α becomes more stable as the plot sizes used to estimate it become larger. This should apply particularly to tropical forests, where the large variability of forest attributes found for small plots is substantially reduced at a scale of 1 ha (Clark and Clark 2000, Chave et al, 2001, Chave et al., 2003, Köhler & Huth, 1998).

The use of allometric equations to derive biomass from Pol-InSAR height will be explored during Phase A of the mission; this will require further work to consolidate allometric relationships for the major forest biomes.

3.2.3 Deriving forest information from SAR tomography

Phase 0 and Phase A include studies on the use of SAR tomography to gain information on the interactions between radar waves and the forest canopies. This technique exploits multi-baseline interferometric SAR observations to reconstruct the scattering from a vegetation layer as a function of height (Reigber and Moreira (2000), Fornaro et al. (2005), Cloude, 2006; Tebaldini and Rocca, 2008). These measurements provide new insight into the physical links between forest biomass and P-band observables, by clarifying the main P-band scattering mechanisms in forest media, their relative contribution to the total radar signal, and their variation over different forest types. Of particular value to the BIOMASS mission is the ability of SAR tomography to distinguish the contributions to the radar signal from the forest canopy (the tree crowns) and from double-bounce scattering, since the scattering geometry causes the latter to appear as a return from ground level. Using the data acquired at the Remningstorp forest, it was found that the relative contribution of the backscatter from ground level is largely dominant for the HH and VV polarisations (the ratio is of the order of 10 dB), and still dominant, though moderately, at HV (of the order of 3 dB) (Tebaldini and Rocca, 2008, Tebaldini, 2010). Figure 8 shows the ratio between the backscatter from the ground and from the canopy for HV polarisation (the same scene as in figs. 4 and 7). The backscatter from the ground level was found higher than that of the canopy level (corresponding to ground-to-canopy ratio >0 dB) in many of the forested areas. This would not be expected from most current scattering models and indicates the need for improved scattering models that take into account the impact of tree structure, understorey and topography.

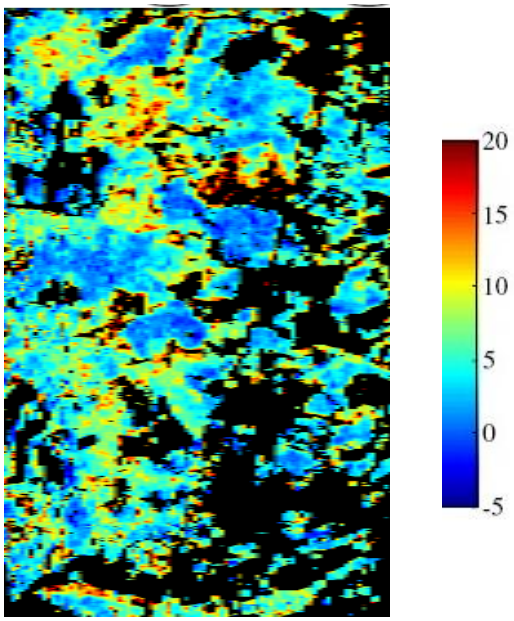

Figure 8*: Ratio of the backscatter from ground level to the backscatter from canopy level at HV with colour scale shown in dB. Non forest pixels are in black. The data are from the same Remningstorp scene as in Figs. 4 and 7.*

SAR tomography therefore leads to better understanding of which processes contribute to the observed SAR signal, and should lead to both improved models of the interaction between radar waves and the forest canopy, and better inversion methods using intensity and Pol-InSAR. During the mission itself, it is proposed to further this process by including a short experimental phase devoted to SAR tomography.

3.3. Exploiting intensity and Pol-InSAR information in biomass recovery

Section 3.1 shows the use of intensity data in biomass retrieval, while Sections 3.2.1 and 3.2.3 respectively illustrate the derivation of canopy height from Pol-InSAR and the retrieval of information on forest structure from SAR tomography. It is of considerable value that these independent types of information can be provided by the same SAR system and combined in biomass retrieval, as is illustrated in Fig. 9 using data from Remningstorp. Here the retrieval is based on linear regression of the mean values of intensity, Pol-InSAR height and tomographic Ground to Volume backscatter ratio derived from 10 reference plots of 80 m x 80 m, where accurate in situ biomass measurements are available. The figure shows the comparison between estimated biomass and in situ biomass for a) inversion of HV intensity data, b) inversion using HV and HH intensity data together with Pol-InSAR height, and c) inversion using HV and HH intensity data, Pol-InSAR height and the Ratio of Ground to Volume backscatter at HV. The RMS error in biomass reduces as more information is added into the inversion, going from 42.3 t ha^{-1} when using just HV intensity (comparable to the inversion result in fig. 4, but with fewer test stands), to 27.9 t ha^{-1} with the addition of HH and Pol-InSAR height, and to 11.0 t ha^{-1} when the tomographic HV ground to canopy backscatter ratio is included. The result in 9c indicates that the structure information provided by tomography enhances the information from Pol-InSAR height.

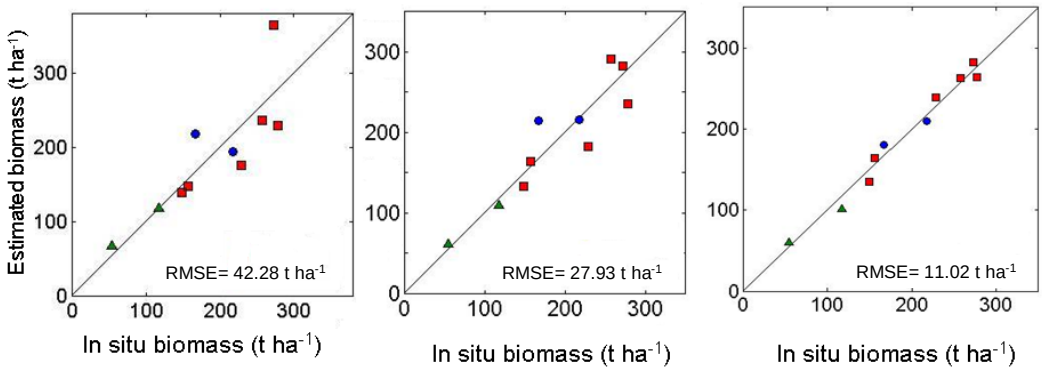

Figure 9: Comparison of estimated and in situ biomass for a) inversion of HV intensity data, b) inversion using HV & HH intensity data together with Pol-InSAR height, and c) inversion using HV & HH intensity data, Pol-InSAR height and the HV Ground to Volume backscatter ratio. Squares: spruce stands, circles: pine stands, and triangles: birch stands.

The inversion techniques are currently being tested on new airborne P-band datasets acquired to assess two important effects: a) the impact of topography on backscatter intensity and Pol-InSAR, and hence on biomass retrieval; this uses data acquired in 2008 from a boreal forest with marked topography; b) the temporal decorrelation in tropical forests over time-intervals comparable with those for a spaceborne system (20-45 days), using data acquired in French Guiana in 2009.

An important aim during the phase A studies is to provide better statistical characterisation of the errors in the inversions. As can be seen from Fig. 2, these errors are likely to depend on the biomass itself, as well as on issues such as system noise, calibration errors and "geophysical" scatter arising from environmental perturbations of the inversion relation. Joint error models are needed that take into account the different measurements, such as intensity data and information derived from Pol-InSAR. This information is important for quantifying not only the uncertainty in the estimated biomass itself, but also how this propagates through carbon cycle estimates which make use of it.

4 Measuring forest biomass change with time

Section 3 has focused on measuring biomass itself, which is of basic importance for quantifying forest resources across the globe, but, as noted in Section 1, *change* in forest biomass is the crucial variable needed for quantifying carbon fluxes and their effects on climate.

The BIOMASS mission will address this by providing consistent and repeated global observations of forests throughout the mission lifetime. These observations will contribute to quantifying the dynamics of forest biomass in three ways:

1) From the time series of estimated biomass in all major forest biomes produced by BIOMASS, the loss of biomass due to stand-removing disturbances can be easily quantified.

2) The increase of biomass due to forest regrowth in the first years after disturbance can be quantified at frequencies ranging from yearly to a single estimate over the whole 5-year mission duration, depending on the forest biome, species and site index (or site quality). In tropical forests, rates of growth can vary from 9 t ha^{-1} yr^{-1} to 21 t ha^{-1} yr^{-1} during the first 10 years of regrowth (Overman et al., 1994, Uhl et al., 1988), Such a differential rate of recovery in the tropics is expected to be quantified by BIOMASS for different recovering areas. Conversely, for regions with very low recovery rate, the 5 year lifetime of BIOMASS may not be sufficient. It is for example the case of Northern Eurasian forests in regions with low site quality which may accumulate in the first years less than 1 t ha^{-1} yr^{-1} (IIASA 2007).

3) Detection and estimation of forest degradation due to selective removal of timber and localised forest clearing requires the capability to detect changes in biomass in mature forest stands. Analysis based on simulated 256-look HH and HV data in inversion indicates that, except for the lowest levels of biomass, changes in biomass of around 30% are detectable with error probability not exceeding 20% (European Space Agency, 2008).

5. Secondary mission objectives

Although the primary focus of the BIOMASS mission is the measurement of forest biomass and its changes, this first chance to explore the Earth's environment with a long wavelength satellite SAR provides major new geoscience opportunities. In

particular, BIOMASS is expected to provide new information on subsurface structure in arid lands and polar ice, to extend existing information on forest inundation, and potentially to provide information on quantities such as soil moisture, permafrost and sea salinity.

5.1 Subsurface geomorphology

Low frequency SAR is able to map the subsurface down to several meters in arid areas, thus has great potential for terrestrial applications, such as hydrology, geology, water and oil resources, and archaeology (Abdelsalam et al., 2000), in arid and semi-arid environments. In particular, the major drainage basins in North Africa are key features for understanding climate change in the recent past, but are very poorly known. Complete coverage of the eastern Sahara was provided by the Japanese JERS-1 L-band satellite, allowing the creation of the first regional-scale radar mosaic covering Egypt, northern Sudan, eastern Libya and northern Chad (Paillou et al., 2009). Such continental-scale exploration is being continued with the PALSAR L-band radar on the JAXA ALOS satellite. Its improved data quality has allowed mapping of a 1200 km-long palaeo-drainage system in eastern Libya that could have linked the Kufrah Basin to the Mediterranean coast (Paillou et al., 2009). Such a major drainage system has important implications for understanding the environments and climates of northern Africa from the Late Miocene to the Holocene, with consequences for fauna, flora, hominid and human dispersal.

These promising results from L-band are likely to be considerably improved by the increased penetration offered at P-band. Using values of dielectric constant that are typical for dry sandy sediments, an L-band SAR would have an expected penetration depth of about 1.3 m, while P-band should penetrate to about 3.7 m. Aircraft campaigns

have in fact demonstrated that P-band SAR can penetrate to at least 4 m in sandy environments (Farr, 2001; Grandjean et al., 2001).

5.2 Sub-surface ice structures and interferometric ice flow measurements

A limitation of shorter wavelength SAR systems (e.g. C-band) for ice studies is their lack of penetration into ice, together with the fact that surface change processes can produce a loss of coherence in interferometric data. It is expected that the P-band signal will penetrate tens of metres of ice, thus reaching larger and more stable scatterers deep under the ice surface. This not only means that subsurface structure can be investigated, but also that interferometric coherence over ice should remain high, allowing the monitoring of glacier displacements over longer time than can be achieved with interferometry at higher frequencies (Mattar et al., 1998, Rignot et al., 2008). A P-band SAR should then be able to fill the time-scale between days and years, providing valuable information about glacier dynamics over periods that correspond to annual change.

5.3 Forest inundation

A basic requirement for modeling methane or carbon dioxide emissions from inundated forests is information on the spatial and temporal distributions of inundated area. The ability of long wavelength radar to map wetland inundation (for example, the Amazon and the Congo basins) has been demonstrated using JERS L-band data (Hess et al., 2003, Martinez and Le Toan, 2007). Using ALOS PALSAR, the timing and duration of flooding over entire catchments have been spectacularly displayed (see http://www.eorc.jaxa.jp/ALOS/kyoto/jan2008/pdf/kc9_hess.pdf). Systematic data acquisition over all the inundated forest areas and the greater penetration into the forest canopy by the BIOMASS sensor mean that it will add substantially to the time-series

being produced by PALSAR and allow the study of decadal trends and inter-annual variations in the dynamics of these very important ecosystems.

6. Mission characteristics

The science requirements of the BIOMASS mission place strong constraints on the characteristics of the space segment. These are briefly discussed in this Section, which pulls together many of the ideas set out in previous sections. A summary is also given in Table 1, and a more complete treatment will be found in the BIOMASS Report for Assessment (European Space Agency, 2008).

Polarimetry. Access to the full range of biomass encountered in the world's forests requires measurement of forest height, and hence a fully polarimetric system in order to support polarimetric interferometry. In addition, direct methods of measuring forest biomass benefit from using intensity measurements at multiple polarisations, and correction of Faraday rotation caused by the ionosphere requires polarimetric data (Bickel and Bates, 1965; Freeman, 2004; Qi and Jin, 2007; Chen and Quegan, 2009).

Resolution. Two considerations underlie the choice of resolution of the BIOMASS sensor. The first is scientific, and is the need to make measurements at a scale comparable to that of deforestation and forest disturbance, i.e. around 1 ha. The second is forced by the ITU allocation of only 6 MHz to P-band for remote sensing, which corresponds to a ground range resolution of around 50 m (depending on the incidence angle). It is envisaged that BIOMASS will provide level-1 products with around 50 m x 50 m resolution at 4 looks. By applying optimal multi-channel filtering techniques to a time-series of HH, HV and VV intensity data, the speckle in each image can be significantly reduced without biasing the radiometric information in each image. For example, a multi-temporal set of six such triplets of intensity data would yield an equivalent number of looks of around 40 or greater at each pixel (Quegan and Yu,

2001), so averaging 2x2 blocks of pixels would yield around 150 looks at a scale of 1 ha, after allowing for inter-pixel correlation. This yields a radiometric accuracy better than 1 dB, which is sufficient to meet the science objectives.

Incidence angle. Airborne experiments have been carried out for incidence angles ranging from 25° to 60°, and most indicate that the preferred incidence angle is in the range 40-45°.However system considerations are expected to favour steeper incidence angles. Currently, the minimum incidence angle is set to >23 degrees. Until now, the effect of incidence angles is not thoroughly addressed. In a study on the sensitivity of the SAR intensity (HV) to biomass (Dubois-Fernandez et al., 2005), similar γ backscatter coefficients were obtained at 23° and at 40° for biomass higher than 50 t ha^{-1}, whereas for lower biomass, the backscatter signal is higher at 23°. This is in line with current research based on airborne SAR tomography (Cf. Section 3.2.3) which suggests that observations at incidence angles of 20°-30° may increase the ground-to-volume ratio, in particular for sparse forests and forests in regions with relief, hence increasing the error in biomass retrieval based only on HV intensity. In this case, algorithms based on a combination of different SAR measurements are required. Quantitative assessment of the effect of incidence angle on the SAR intensity, SAR polarimetry, and on PolInSAR and tomography is currently undertaken in the mission phase A, aiming at consolidating the choice of incidence angle and at improving the retrieval algorithms.

Revisit time. Forest height recovery using Pol-InSAR requires a revisit time small enough to maintain high temporal coherence between successive SAR acquisitions. Although this issue is still being investigated, preliminary results suggest that a time interval of between 25-45 days is acceptable.

Orbit. A sun-synchronous dawn-dusk orbit will minimise ionospheric disturbances (Quegan et al., 2008).

Mission duration. A 5-year mission is planned in order to obtain repeated measurements of the world's forests. This will lead to reduced uncertainties in measurements of the biomass of undisturbed forests and will allow measurement of forest dynamics by detecting changes in biomass and forest cover. Although the regrowth of fast-growing tropical forests may be detectable even with measurements spaced one or two years apart, measurement of regrowth in temperate forests requires as long a mission as possible. BIOMASS will have very limited capability for measuring regrowth in the slowly-growing boreal forests.

Tomography. The mission is expected to include a short tomographic phase during which measurements with 10-12 spatial baselines and a revisit time of 1-4 days will be collected.

7. Summary and Conclusions

At present, the status, dynamics and evolution of the terrestrial biosphere are the least understood and the most uncertain elements in the global carbon cycle, which is deeply imbedded in the functioning of the Earth system and its climate. There are very large uncertainties in the distribution of carbon stocks and carbon exchange, in the estimates of carbon emissions due to land use change, and in the uptake of carbon due to forest regrowth. Forest biomass is the main repository of vegetation carbon and hence is a crucial quantity needed to reduce these uncertainties. Both its spatial distribution and its change with time are critical for improved knowledge of the terrestrial component of the carbon cycle.

Although the need is great and urgent, there are no current biomass datasets that are global, up-to-date, consistent, at spatial resolutions comparable with the scales of land use change, or that are systematically updated to track biomass changes due to land use change and regrowth. The BIOMASS mission is designed to address this severe

limitation in our knowledge of the Earth and its functioning. It will aid in building a sustained global carbon monitoring system that improves over time, thus helping nations to quantify and manage their ecosystem resources, and to improve national reporting. Its value will also extend well beyond the mission lifetime: since biomass in undisturbed forest changes relatively slow, the maps produced during the mission will provide realistic values for calculations of emissions based on deforestation maps produced by other means, such as optical or shorter wavelength radar sensors.

The design of the BIOMASS mission is driven by science needs, and spins together two main observational strands: (1) the long heritage of airborne observations in tropical, temperate and boreal forest that have demonstrated the unique capabilities of P-band multi-polarised SAR for measuring the world-wide range of forest biomass; (2) new developments in recovery of forest height from Pol-InSAR, and, crucially, the resistance of P-band to temporal decorrelation, which makes this frequency uniquely suitable for biomass measurements with a single repeat-pass satellite. These two complementary measurement approaches are combined in the single BIOMASS sensor, and have the satisfying property that increasing biomass reduces the sensitivity of the former approach while increasing the sensitivity of the latter. During phase A of the mission, the inversion methods are consolidated using new experimental data acquired over forests with marked topography and over forests with very high biomass density.

However, the BIOMASS P-band radar appears to be the only sensor capable of providing the urgently needed global knowledge about biomass. It seizes the new opportunity from the allocation of a P-band frequency band for remote sensing by the ITU in 2003. It also will be a major addition to current efforts to build a global carbon data assimilation system (Ciais et al., 2003) that will harness the capabilities of a range of satellites and in situ data. It is within this context that BIOMASS will find its fullest

expression, both gaining from and complementing what can be learnt from other satellite systems, ground data, and carbon cycle models.

References

Abdelsalam, M. G., Robinson, C., El-Baz, F., & Stern, R. J. (2000). Applications of orbital imaging radar for geologic studies in arid regions: The Saharan testimony. *Photogrammetric Engineering and Remote Sensing*, *66*, no. 6, 717-726.

Alves D S, Soares J V, Amaral. S, et al., (1997)" Biomass of primary and secondary vegetation in Rondonia, Western Bazilian Amazon. Global Change Biology, 3, 451-461.

Askne, J., Dammert, P. B., Ulander, L. M., & Smith, G. (1997). C-Band repeat-pass interferometric SAR observations of the forest. *IEEE Transactions on Geoscience and Remote Sensing*, *35*, no. 1, 25-35.

Beaudoin, A., Le Toan, T., Goze, S., Nezry, E., Lopes, A, et al. (1994). Retrieval of forest biomass from SAR data. *International Journal of Remote Sensing*, *15*, 2777-2796.

Beer, C., Lucht, W., Schmullius. C., & Shvidenko, A. (2006). Small net uptake of carbon dioxide by Russian forests during 1981-1999. *Geophysical Research Letters*, *33*: L15403-doi:10.1029/2006GL026919.

Bickel, S. H. and Bates, R. H. T. (1965). Effects of magneto-ionic propagation on the polarization scattering matrix. *Proc. IRE,* vol. 53, 1089-1091.

Bunker, D. E., DeClerck, F., Bradford, J. C., Colwell, R. K., Perfecto, I., et al. (2005). Species loss and aboveground carbon storage in a tropical forest. *Science*, *310*, no. 5750, 1029-1031.

Canadell, J. G., Le Quéré, C., Raupach, M. R., Field, C.B, Buitehuis, E. T., et al. (2007) Contributions to accelerating atmospheric CO_2 growth from economic activity, carbon intensity, and efficiency of natural sinks. *Proceedings of the National Academy of Science, 104*, 18866–18870.

Ciais, P., Moore, B., Steffen, W., Hood, M., Quegan, S., et al. (2003). *Final Report on the IGOS-P Carbon Theme, The Integrated Global Carbon Observing Strategy: A Strategy to Build a Coordinated Operational Observing System of the Carbon Cycle and its Future Trends*, FAO.

Chave, J., Riéra, B., & Dubois, M.A. (2001). Estimation of biomass in a neotropical forest of French Guiana: spatial and temporal variability. *Journal of Tropical Eco*logy, *17*, 79-96. •

Chave,J, Chust,G., Condit R., Aguilar S., Lao S., Perez R. 2004. Error propagation and scaling for tropical forest biomass estimates. *Philosophical Transactions of the Royal Society of London B* 359, 409-420.

Chave, J., Condit, R., Lao, S., Caspersen, J. P., Foster, R. B., et al. (2003). Spatial and temporal variation in biomass of a tropical forest: results from a large census plot in Panama. *Journal of Ecology, 91*, 240-252.

Chen, J. and Quegan, S. (2009). Improved estimators of Faraday rotation using spaceborne polarimetric SAR data. *IEEE Trans. Geosci. Remote Sens. Letts.* (under review).

Clark, D. B. & Clark, D. A. 2000 Landscape-scale variation in forest structure and biomass in a tropical rain forest. *Forest Ecol. Mngmt* **137**, 185–198.

Cloude, S. R. & Papathanassiou, K. P. (1998). Polarimetric SAR interferometry. *IEEE Transactions on Geoscience and Remote Sensing*, *36*, no. 5, 1551-1565.

Cloude, S. R., Papathanassiou, K. P. & Pottier, E. (2001). Radar polarimetry and polarimetric interferometry. *IEICE Transactions on Electronics*, *E84-C*, no. 12, 1814-1822

Cloude, S. R. (2006). Polarisation coherence tomography. *Radio Science*, *41*, RS-4017.

Dubois-Fernandez, P., Champion, I., Guyon D., Cantalloube H., Garestier F., Dupuis X., Bonin G., Forest biomass estimation from P-band high incidence angle data. Proceedings PolInSAR workhop, ESA 2005 http://earth.esa.int/workshops/polinsar2005/participants/88/paper_Biomass_estimation_from_Pband.PDF

Dubois-Fernandez, P., Souyris, J. C., Angelliaume, S., & Garestier, F. (2008). The compact polarimetry alternative for spaceborne SAR at low frequency. *IEEE Transactions on Geoscience and Remote Sensing*, *46*, no.10.

DeFries, R. S., Houghton, R. A., Hansen, M. C., Field, C. B., & Skole, D. (2002). Carbon emissions from tropical deforestation and regrowth based on satellite observations for the 1980s and 1990s. *Proceedings of the National Academy of Science*, *99*, 14256-14261.

Dobson, M. C., Ulaby, F. T., Le Toan, T., Beaudoin, A., Kasischke, E., e al. (1992). Dependence of radar backscatter on coniferous forest biomass. *IEEE Transactions on Geoscience and Remote Sensing*, *30*, no. 2, 412-415.

European Space Agency (2008). *BIOMASS Report for Assessment*. ESA SP 1313/2, European Space Agency.

FAO (2001). *Global Forest Resources Assessment 2000, Main Report,* FAO Forestry Paper 140, FAO, Rome.

FAO (2006). *Global Forest Resources Assessment 2005*, FAO Forestry Paper 147, FAO, Rome.

Farr, T. (2001). Imaging radar in the Mojave desert – Death Valley region. *Proceedings of Workshop on the Martian highlands and Mojave desert analogs,* Las Vegas, USA.

Ferrazzoli, P., Paloscia, S., Pampaloni, P., Schiavon, G., Sigismondi, S. et al. (1997). The potential of multifrequency polarimetric SAR in assessing agricultural and arboreous biomass. *IEEE Transactions on Geoscience and Remote Sensing***,** *35* , no. 1,

Freeman, A. (2004). Calibration of linearly polarized polarimetric SAR data subject to Faraday rotation, *IEEE Transactions on Geoscience and Remote Sensing*, *42,* Aug..2004.

Fung, A..K. (1994). *Microwave Scattering and Emission Models and their Applications*. Artech House.

Garestier, F., Dubois-Fernandez. P. & Papathanassiou, K. P. (2008a). Pine forest height inversion using single pass X-band Pol-InSAR data. *IEEE Transactions on Geoscience and Remote Sensing*, *46,* no. 1.

Garestier, F., Dubois-Fernandez, P., & Champion, I. (2008b). Forest height inversion using high resolution P-band Pol-InSAR data. *IEEE Transactions on Geoscience and Remote Sensing*, **46**, no. 10.

Garestier, F., & Le Toan, T. (2009)a. Forest modeling for height inversion using InSAR/Pol-InSAR data. *IEEE Transactions on Geoscience and Remote Sensing*. In press, December 2009.

Garestier, F., & Le Toan, T. (2009)b. Estimation of the backscatter vertical profile of a pine forest using single baseline P-band (Pol-) InSAR data. *IEEE Transactions on Geoscience and Remote Sensing*. Accepted, December 2009.

GCOS (2003). *Second report on the Adequacy of the Global Observing System for Climate in Support of the UNFCCC*, GCOS–82 (WMO/TD No. 1143), World Meteorological Organization, 74 pp.

G. Grandjean, Ph. Paillou, P. Dubois, T. August-Bernex, N. Baghdadi, J Achache, "Subsurface structures detection by combining L-band polarimetric SAR and GPR data: Example of the Pyla Dune (France)", IEEE Transactions on Geoscience and Remote Sensing, vol. 39, no. 6, pp. 1245-1258, 2001.

Haberl, H., & Erb K.-H. (2006). Assessment of sustainable land use in producing biomass. In: *Renewables-Based Technology: Sustainability Assessment* (eds. Dewulf, J., & Langenhove, H. V.) Chichester: John Wiley & Sons, 175-192.

Hajnsek, I., Kugler, F., Lee, S.-K. & Papathanassiou, K. P. (2009). Tropical forest parameter estimation by means of Pol-InSAR: The INDREX-II Campaign. *IEEE Transactions on Geoscience and Remote Sensing*, Vol. 47, no 2, February 2009..

Hess L.L., Melack J. , Evlyn M.L.M. Novo E., Barbosa C., Gastil M.,Dual-season mapping of wetland inundation and vegetation for the central Amazon basin Remote Sensing of Environment, 87 (2003) 404-428

Herold, M., Brady, M., Wulder, M., & Kalensky, D. (2007). Biomass. In: *Terrestrial Essential Climate Variables for Climate Change Assessment, Mitigation and Adaptation, GTOS Biennial report supplement, Report of the Global Terrestrial Observing System (GTOS) Nr. 52*, URL: www.fao.org/gtos, 34-35.

Hoekman, D. H. & Quinones, M. J. (2000). Land cover type and biomass classification using AirSAR data for evaluation of monitoring scenarios in the Colombian Amazon. *IEEE Transactions on Geoscience and Remote Sensing*, *38*, no. 2, 685-696.

Houghton, R. A., Lawrence, K. T., & Hackler, J. L. (2003). The spatial distribution of forest biomass in the Brazilian Amazon: a comparison of estimates. *Global Change Biology*, *7*, 731-746.

Houghton, R. A. (2003a). Revised estimates of the annual net flux of carbon to the atmosphere from changes in land use and land management 1850-2000. *Tellus*, *55B(2),* 378–390.

Houghton, R. A. (2003b). Why are estimates of the terrestrial carbon balance so different? *Global Change Biology*, *9(4)*, 500-509.

Houghton, R. A. (2005). Aboveground forest biomass and the global carbon cycle. *Global Change Biology, 11*, 945-958.

Hsu, C. C., Han, C., Shin, R. T., Kong, J. A., Beaudoin, A., et al. (1994). Radiative transfer theory for polarimetric remote sensing of pine forest at P-band. *International Journal of Remote Sensing, 15*, 2943-2954.

IIASA 'Russian Forest and Forestry' 2007 in www.iiasa.ac.at.

IPCC (2007). *Climate Change 2007: the Physical Basis. Working Group I Contribution to the Fourth Assessment Report of the Intergovernmental Panel on Climate Change* (eds. Solomon, S., Qin, D., Marquis, M., Averyt, K. B., Tignor, M., et al.). Cambridge University Press, Cambridge UK and New York, NY, USA, 996 pp.

IPCC (2003). *Good Practice Guidance for Land Use, Land Use Change and Forestry* (eds. Penman, P., Gytarsky, M., Hiraish, T., Krug, T., Kruger, D., et al.). The Intergovernmental Panel on Climate Change.

ITU-2004, *Article 5 ("Frequency Allocations") of the Radio Regulations*, Edition 2004, International Telecommunication Union.

Kindermann, G. E., McCallum, I., Fritz, S., & Obersteiner, M. (2008). A global forest growing stock, biomass and carbon map based on FAO statistics. *Silva Fennica, 42(3)*, 387-396.

Köhler, P., & Huth, A. (1998). The effect of tree species grouping in tropical rain forest modelling: Simulation with the individual based model Formind. *Ecological Modelling, 109*, 301–321.

Krausmann, F., Erb, K.-H., Gingrich, S., Lauk, C., & Haberl, H. (2008). Global patterns of socioeconomic biomass flows in the year 2000: A comprehensive assessment of supply, consumption and constraints. *Ecological Economics, 65(3),* 471-487.

Kugler, F., Koudougbo, F., Papathanassiou, K. P., Hajnsek, I. & Hoekman D. H. (2006). Frequency effects in Pol-InSAR forest height estimation. *Proceedings of EUSAR 2006*, Dresden, 16-18 May.

Kugler, F., Papathanassiou, K. P., Hajnsek, I., Hoekman, D. H. (2006). Forest height estimation in tropical rain forest using Pol-InSAR techniques. *Proceedings of the IEEE International Geoscience and Remote Sensing Symposium 2006 (IGARSS 2006),* 31 July - 4 August, Denver, USA.

Le Quéré C et al. (2009) Trends in the sources and sinks of carbon dioxide. Nature Geoscience doi:10.1038/ngeo689.

Le Toan, T., Beaudoin, A., Riom, J. & Guyon, D. (1992). Relating forest biomass to SAR data, *IEEE Transactions on Geoscience and Remote Sensing*, *30,* 403-411.

Le Toan T, Quegan S, Woodward FI, Lomas MR & Delbart N (2004) Relating radar remote sensing of biomass to modelling of forest carbon budgets. Climatic Change, 67, 379-402.

Lee, S.-K., Kugler, F., Papathanassiou, K. P. & Hajnsek I. (2008) Quantifying temporal decorrelation over boreal forest at L- and P-band. *7th European Conference on Synthetic Aperture Radar (EUSAR 2008)*, Friedrichshafen, Germany, 2–5 June.

Malhi, Y. & Phillips, O. L. (2004). Tropical forests and global atmospheric change: a synthesis. *Philosophical Transactions of the Royal Society, 359*, no. 1443, 549-555.

Malhi, Y., Wood, B., Baker, T. R., Wright, J., Phillips, O. L., et al. (2006). The regional variation of aboveground live biomass in old-growth Amazon forests. *Global Change Biology*, 12, 1-32.

Martinez J. M. and Le Toan T. "Mapping of Flood Dynamics and Spatial Distribution of Vegetation in the Amazon Floodplain Using Multitemporal SAR Data" Remote Sensing of Environment,108,(3), 209-223,(2007).

K.E. Mattar, P.W. Wachon, D. Gedtner, A.L. Gray, I.G. Cumming, M. Brugman, Validation of alpine glacier velocity measurements using ERS tandem-mission SAR data, IEEE Trans. Geosc. Rem. Sens., vol. 36, no. 3, 1998.

Mette, T., Papathanassiou, K. P., Hajnsek, I., Pretzsch, H., & Biber, P. (2004). Applying a common allometric equation to convert height from Pol-InSAR data to forest biomass. *Proceeding of IEEE Geoscience and Remote Sensing Symposium 2004 (IGARSS 2004)*, 20. - 24. September, Anchorage, Alaska,

Myneni R. B., Dong, J., Tucker, C. J., Kaufmann, R. K., Kauppi, P. E., et al. (2001). A large carbon sink in the woody biomass of Northern forests. *Proceedings of the National Academy of Sciences (PNAS), 98*, no. 6, 14784-14789.

Olson, J. S., Watts, J. A. & Allison, L. J. (1983). *Carbon in Live Vegetation of Major World Ecosystems*. Report ORNL-5862. Oak Ridge National Laboratory, Oak Ridge, Tennessee. 164pp.

Olson, D. M., Dinerstein, E., Wikramanayake, E. D., Burgess, N. D., Powell, G. V. N., et al. (2001). Terrestrial ecosystems of the world: a new map of life on earth. *Bioscience*, *51(11)*, 933-938.

Overman JPM, Witte HJL, Saldarriaga JG (1994) Evaluation of regression models for above-ground biomass determination in Amazon rain forests. journal of tropical Ecology, 10, 207-218.

Paillou, P., & Dreuillet, P. (2002). The PYLA'01 experiment: Flying the new RAMSES P-band facility. *Proceedings of the AIRSAR Earth Science and Application Workshop 2002*, Pasadena, USA.

Paillou, P., S. Lopez, T. Farr, A. Rosenqvist, "Mapping Subsurface Geology in Sahara using L-band SAR: Potential for Detection of Water Resources", IEEE J. of Selected Topics in Earth Observations and Remote Sensing, 2009, submitted.

Ph. Paillou, M. Schuster, T. Farr, S. Tooth, A. Rosenqvist, S. Lopez, J.-M. Malézieux, "Mapping of a major paleodrainage system in Eastern Libya using orbital imaging Radar: The Kufrah River", Earth and Planetary Science Letters, vol. 277, pp. 327-333, doi: 10.1016/j.epsl.2008.10.029, 2009.

Papathanassiou, K. P., & Cloude, S. R. (2001). Single baseline polarimetric SAR interferometry. *IEEE Transactions on Geoscience and Remote Sensing*, *39*, no. 11, 2352-2363.

Praks, J., Kugler, F., Papathanassiou, K. P., Hajnsek, I., & Hallikainen, M. (2007). Height estimation of boreal forest: interferometric model based inversion at L- and X-band vs. HUTSCAT profiling scatterometer. *IEEE Geoscience and Remote Sensing Letters*, *4*, no 3, 466 – 470.

Qi R-Y and Jin Y-Q (2007) Analysis of the effects of Faraday rotation on spaceborne polarimetric SAR observations at P-band. *IEEE Trans. Geosci. Remote Sens.*, vol. 45, no. 5, 1115-1122.

Quegan, S. & Yu, J. J. (2001). Filtering of multichannel SAR images. *IEEE Transactions on Geoscience and Remote Sensing*, *39*, no. 11, 2373-2379.

Quegan S., Green, J. J., Zandona-Schneider, R., Scheiber, R., & Papathanassiou, K. P. (2008). Quantifying and correcting ionospheric effects on P-band SAR images. *Proceeding of IEEE Geoscience and Remote Sensing Symposium 2008 (IGARSS 2008)*, July 6-11, Boston, USA.

Ranson, K,.J., & Sun, G. (1994). Mapping biomass of a northern forest using multifrequency SAR data. *IEEE Transactions on Geoscience and Remote Sensing*, *32*, 388-396.

Rignot, E. J., Way, J., Williams, C., & Viereck, L. (1994). Radar estimates of aboveground biomass in boreal forests of interior Alaska. *IEEE Transactions on Geoscience and Remote Sensing*, *32*, no. 5, 1117-1124.

E. Rignot, J.L. Bamber, M.R. van den Broeke, C. Davis, Y. Li, W. Jan van de Berg, E. van Meijgaard, Recent Antarctic ice mass loss from Radar interferometry and regional climate modelling, Nature Geoscience vol. 1, pp. 106-110, 2008.

Saatchi SS, Halligan K, Despain DG and Crabtree RL (2007) Estimation of forest fuel load from radar remote sensing. *IEEE Trans. Geosci. Remote Sensing*, 45, no. 6, 1726-1740.

Saatchi, S., Marlier, M., Chazdon, R., Clark, D., and A. Russell, (2009). Impacts of spatial variability and scale on radar estimation of structure and above-ground biomass in tropical forests, *JGR, Biogeosciences* (under review).

G. Sandberg, L. M. H. Ulander, J. E. S. Fransson, J. Holmgren and T. Le Toan (2009), 'L-band versus P-band SAR for biomass retrieval in semi-boreal forest'. *Remote Sensing of Environment* (Accepted, Remote Sensing of Environment ,December 2009)

Schmullius, C., Baker, J., Balzter, H., Davidson, M., Gaveau, D. M. Gluck, A. Holz, T. Le Toan, A. Luckman, U. Marschalk, S. Nilsson, S. Quegan, et al., (2001). *SIBERIA – SAR Imaging for Boreal Ecology and Radar Interferometry Applications*, European Commission 4th Framework Project ENV4-CT98-0743 (DG12-EHKN), Final Report, September 2001.

Sessa, R., & Dolman, H. (eds.) (2008). *Terrestrial Essential Climate Variables for Climate Change Assessment, Mitigation and Adaptation*, GTOS-52, FAO, Rome.

Smeets, E. M. W., & Faaij, A. P. C. (2007). Bioenergy potentials from forestry in 2050. *Climatic Change, 81(3)*, 353-390.

Tebaldini (2009): Algebraic synthesis of forest scenarios from multibaseline polinsar data. Geoscience and Remote Sensing, IEEE Transactions on, 47(12):4132–4142, Dec. 2009.

Tebaldini, S. (2010): Single and Multi Polarimetric SAR tomography of forested Areas: a parametric approach. Accepted for publication on IEEE Transactions on Geoscience and Remote Sensing

Tebaldini, S. & Rocca, F. (2008). Polarimetric SAR tomography of forested area: a covariance matching approach. *Proceedings of EuSAR* 2008.

Treuhaft, R. N. & Siqueira, P. R. (2000). The vertical structure of vegetated land surfaces from interferometric and polarimetric radar. *Radio Science, 35*, no. 1, 141-177.

Ulaby, F.T., Sarabandi, K., McDonald, K., Whitt, M., & Dobson, M.C. (1990). Michigan microwave canopy scattering model. *International Journal of Remote Sensing, 11*, 1223-1254.

Uhl. C, Buschbacher R, Serrao EAS (1988) Abandoned pastures in Eastern Amazonia, Journal of Ecology, 76, 663-681.

Whiteman, A., Broadhead, J., & Bahdon, J. (2002). The revision of woodfuel estimates in FAOSTAT. *Unasylva, 53(211)*, 41-45.

Woodhouse, I. H. (2006). Predicting backscatter-biomass and height-biomass trends using a macroecology model. *IEEE Transactions on Geoscience and Remote Sensing, 44*, no. 4, 871-877.